

# Thermodynamic Performance Improvement of Recompression Brayton Cycle Utilizing CO<sub>2</sub>-C<sub>7</sub>H<sub>8</sub> Binary Mixture

Muhammad Ehtisham SIDDIQUI

Mechanical Engineering Department, King Abdulaziz University, Jeddah 21589, Saudi Arabia,

E-mail: mesiddiqui@kau.edu.sa

**crossref** <http://dx.doi.org/10.5755/j02.mech.28126>

## Nomenclature

BC – Brayton cycle;  $\dot{E}_{g,air}$  – Exergy gain by the cooling air in the cooler;  $\dot{E}_{in}$  – Input exergy;  $\dot{E}_j$  – Exergy of the working fluid at  $j^{th}$  State;  $\dot{E}_{l,cooler}$  – Exergy loss in the cooler;  $\dot{E}_{l,fluid}$  – Exergy loss by the working fluid in the cooler;  $\dot{E}_{l,T}$  – Exergy loss in the turbine;  $\dot{E}_{l,C1}$  – Exergy loss in the compressor C1;  $\dot{E}_{l,C2}$  – Exergy loss in the compressor C2;  $\dot{E}_{l,HTR}$  – Exergy loss in the HTR;  $\dot{E}_{l,LTR}$  – Exergy loss in the LTR; EoS – Equation of state; GWP – Global Warming Potential; HTR – High Temperature Recuperator; LTR – Low Temperature Recuperator; ODP – Ozone Depletion Potential;  $\dot{Q}_{in}$  – Heat input to the cycle; RBC – Recompression Brayton Cycle; S-CO<sub>2</sub> – Supercritical carbon dioxide;  $T_a$  – Ambient temperature;  $TIT$  – Turbine Inlet Temperature;  $T_s$  – Source temperature; VLE – Vapor-liquid equilibrium;  $\dot{W}_{C1}$  – Power consumption by compressor C1;  $\dot{W}_{C2}$  – Power consumption by compressor C2;  $\dot{W}_{C,net}$  – Net power consumption by compressors;  $\dot{W}_T$  – Turbine power output;  $\varepsilon_{HEX}$  – Heat exchanger effectiveness;  $\eta_{th}$  – Thermal efficiency.

## 1. Introduction

Increasing demand of electrical power raises a global concern due to rapid depletion of fossil fuel. Therefore, efficient conversion of heat to power is much needed than ever before. Power generation systems utilizing low grade waste heat or renewable sources are getting much attention due to their potential to improve the efficiency of the plant and ultimately reducing the harm caused to the environment.

A literature survey shows increasing research interest in supercritical carbon dioxide (S-CO<sub>2</sub>) Brayton cycle (BC). Recompression BC layout using CO<sub>2</sub> as a working fluid was initially proposed in 1968 by Feher and Angelino reporting higher thermal efficiencies for low to medium temperature sources [1, 2]. Many configurations of Brayton cycle using S-CO<sub>2</sub> as a working fluid are found in the literature for various heat sources and applications from nuclear to solar [3-6].

The cycle essentially takes the advantage of the thermodynamic properties of CO<sub>2</sub> pertaining to its critical point ( $T_{cr} = 31^\circ\text{C}$ ,  $P_{cr} = 7.38\text{ MPa}$ ). Maintaining the state of CO<sub>2</sub> near its critical point at the inlet of compressor significantly reduces the compression work, ultimately improving

the overall efficiency of the cycle. However, operating S-CO<sub>2</sub> BC in high ambient temperature regions poses a problem of cooling CO<sub>2</sub> to its critical temperature, hence, adversely affecting the thermal efficiency of the cycle. This issue can be managed by raising the critical temperature using CO<sub>2</sub> based binary mixture [7, 8].

Invernizzi et al. studied various additives for CO<sub>2</sub> to operate BC and found substantial improvement in the thermal efficiency of the cycle [9]. Later Invernizzi extended the investigation and suggested the possibility of various additives for CO<sub>2</sub> based binary mixtures [10]. For warmer regions, Seungjoon et al. performed preliminary study on the selection of additives for s-CO<sub>2</sub> power cycles with R-123, R-134a, R-22, R-32, C<sub>7</sub>H<sub>8</sub>, and SF<sub>6</sub>. They concluded that the BC perform better thermodynamically when using CO<sub>2</sub>-R32 and CO<sub>2</sub>-C<sub>7</sub>H<sub>8</sub> binary mixtures as working fluids instead of pure CO<sub>2</sub> [11]. Using solar energy as a heat source, Manzolini et al. observed that BC utilizing CO<sub>2</sub>-N<sub>2</sub>O<sub>4</sub> and CO<sub>2</sub>-TiCl<sub>4</sub> binary mixture has better thermodynamic performance than conventional steam Rankine cycle [8].

Recently, Haroon et al. performed detailed exergo-environmental and economic analyses of the simple regenerative and partial heating bottoming cycles using CO<sub>2</sub>-C<sub>7</sub>H<sub>8</sub> binary mixtures as working fluid [12, 13]. They performed analyses for warm ambient conditions and concluded that the gain in energetic and exergetic performances are higher for simple regenerative cycle than partial heating cycle. The main source of exergy destruction in the cycles were heat exchangers.

The literature review shows numerous studies in recent past highlighting CO<sub>2</sub>-based binary mixtures for power generation cycles operating in warm ambient conditions. This work is an effort to increase understanding and exploit the role of CO<sub>2</sub>-based binary mixtures in supercritical Brayton cycles. In the current study, a recompression Brayton cycle, RBC, layout is chosen due to its better thermodynamic performance in comparison to various other layouts, like, compression cycle, simple regenerative cycle, or partial heating cycle. Energy and exergy performances of the cycle are investigated with cycle minimum temperature equal to 50°C.

Energy analysis of RBC with pure CO<sub>2</sub>, operating above critical point, is presented first, and the results are validated with the data available in the literature. The effect of cycle minimum temperature on its performance is also discussed. The selection of additive is a challenging process and the appropriate selection of additive depends on multiple factors, like, source temperature, turbine inlet temperature, ambient temperature, and environmental concerns.

Toluene ( $C_7H_8$ ) is selected as an additive for  $CO_2$ -based binary mixture. The selection is based on the favourable recommendations found in the literature. Energetic and exergetic analysis of recompression Brayton cycle operating with pure  $CO_2$  and  $CO_2$ - $C_7H_8$  binary mixture are presented to compare the efficacy of the two working fluids for the regions with warm ambient temperatures.

## 2. $CO_2$ - $C_7H_8$ binary mixture properties

Literature highlights the possibility of multiple additives for  $CO_2$ -based binary mixture [9-14]. Toluene ( $C_7H_8$ ) is selected in this study due to its stability and compatibility with  $CO_2$ , moreover, its small concentration raises the critical temperature of the mixture to the desired level, thus elevating the sink temperature to help cooling process in hot environments [15]. It has low GWP, zero ODP and thermally stable up to  $400^\circ C$  [16].

The study is carried out in Aspen HYSYS utilizing Peng-Robinson (PR) equation of state (EoS) to calculate thermodynamic properties. To validate the model, the vapor-liquid equilibrium (VLE) data is obtained for  $CO_2$ - $C_7H_8$  binary mixture at  $50^\circ C$  and plotted in Fig. 1 along with experimental data [15-17]. It is evident from these plots that the model works reasonably well.

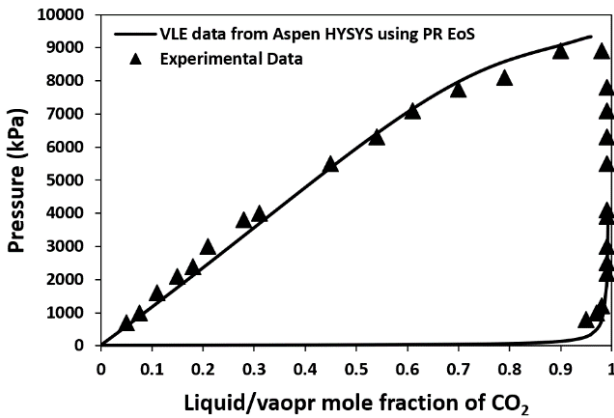


Fig. 1 VLE diagram of  $CO_2$ - $C_7H_8$  binary mixture at  $50^\circ C$ . Experimental data from [15-17] is plotted for the validation of the model

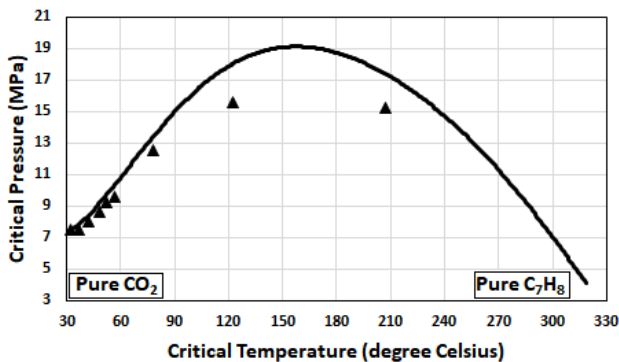


Fig. 2 VLE diagram of  $CO_2$ - $C_7H_8$  binary mixture at  $50^\circ C$ . Experimental data from [15-17] is plotted for the validation of the model

Fig. 2 represents the plot of critical temperature versus critical pressure of  $CO_2$ - $C_7H_8$  binary mixture obtained from Aspen HYSYS and compared with available experimental data. The plot shows a good agreement of the

simulated data with the experimental data for mixture compositions near the critical point of pure  $CO_2$  from critical temperature of pure  $CO_2$  till nearly  $70^\circ C$ . The deviation from the experimental data is apparent at higher concentration levels of  $C_7H_8$  that are not considered in this study.

## 3. S- $CO_2$ Brayton cycle

Owing to the high thermal efficiency for medium to high temperature source, various configurations of recompression Brayton cycle (RBC), with pure  $CO_2$  operating above its critical point, have been studied extensively in past few decades [3, 18-23]. The RBC layout chosen for the current study is shown in Fig. 3. In this layout, there are two compressors and two heat recuperators. After leaving the turbine at state 2, the working fluid experiences two consecutive heat recuperation processes, first in the high temperature recuperator (HTR) and then in the low temperature recuperator (LTR). After leaving LTR, the stream splits into two, one goes to the "Cooler" where it rejects heat to the sink and then compressed in compressor "C1" to cycle's high pressure. Air is used as a coolant for the cooling purpose. The stream leaving C1 is preheated in LTR before it is mixed with the second stream leaving the compressor "C2". The mixed stream at state 9 recovers heat in HTR prior to heating in the Heat Source to desired turbine inlet temperature ( $TIT$ ).

In the first part of the current study, the RBC layout shown in Fig. 3 is investigated with pure  $CO_2$  operating above its critical point. The results obtained from simulation are validated with the literature and the effect of cycle's minimum temperature on the thermal efficiency is studied.

The second part investigates the thermodynamics improvements resulting from  $CO_2$ - $C_7H_8$  binary mixture. Finally, energy and exergy performances of both cases are discussed.

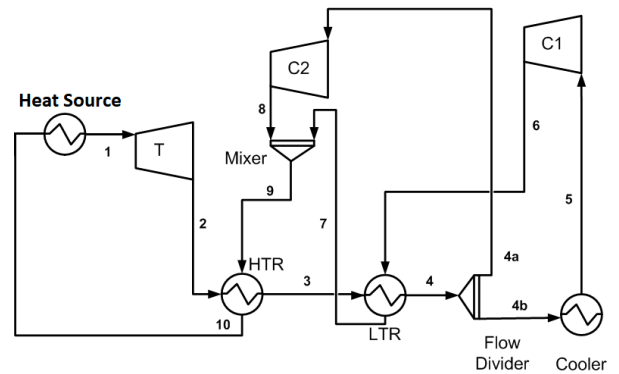


Fig. 3 Recompression Brayton cycle configuration

## 4. Energy model

Energy efficiency of the cycle shown in Fig. 3 is calculated as:

$$\eta_{th} = \frac{\dot{W}_T - \dot{W}_{C,net}}{\dot{Q}_m} \quad (1)$$

where:  $\dot{W}_T$ ,  $\dot{W}_{C,net}$  and  $\dot{Q}_m$  represent turbine power output, net power consumed by both compressors and heat input to the cycle, respectively.

The heat exchanger effectiveness  $\epsilon_{HEX}$  is defined

for total hot stream as [24, 25]:

$$\varepsilon_{HEX} = \frac{h_2 - h_4}{h_2 - h_{4c}}, \quad (2)$$

where:  $h_2$  and  $h_4$  are enthalpies of hot stream at the inlet of HTR and outlet of LTR, respectively;  $h_{4c}$  is the enthalpy of the hot stream at the outlet of LTR based on the inlet temperature of cold side stream. Therefore, in our case,  $h_{4c}$  is the enthalpy of the working fluid at pressure of state point 4 and temperature of state point 6.

### 5. Exergy model

Exergy analysis is done by calculating exergy losses in all the components of the cycle. Exergy of the working fluid at any given state  $\dot{E}_j$  is defined as:

$$\dot{E}_j = \dot{m}_j (h_j - T_a s_j), \quad (3)$$

where:  $\dot{m}_j$ ,  $h_j$  and  $s_j$  represent mass flow rate, enthalpy, and entropy of  $j^{\text{th}}$  state point;  $T_a$  is the ambient temperature in Kelvin. Exergy input  $\dot{E}_{in}$  to the cycle can be computed as:

$$\dot{E}_{in} = \dot{Q}_{in} \left( 1 - \frac{T_a}{T_s} \right), \quad (4)$$

where:  $T_s$  denotes the source temperature (in Kelvin) and is defined as:

$$T_s = (TIT + 273.15) + 50. \quad (5)$$

Losses due to irreversibility's in each component of the cycle are calculated as:

$$\dot{E}_{l,T} = (\dot{E}_1 - \dot{E}_2) - \dot{W}_T, \quad (6)$$

$$\dot{E}_{l,C1} = \dot{W}_{C1} - (\dot{E}_6 - \dot{E}_5), \quad (7)$$

$$\dot{E}_{l,C2} = \dot{W}_{C2} - (\dot{E}_8 - \dot{E}_{4a}), \quad (8)$$

$$\dot{E}_{l,HTR} = (\dot{E}_2 - \dot{E}_3) - (\dot{E}_{10} - \dot{E}_9), \quad (9)$$

$$\dot{E}_{l,LTR} = (\dot{E}_3 - \dot{E}_4) - (\dot{E}_7 - \dot{E}_6). \quad (10)$$

Cooler is air cooled and the exergy gain by the cooling air, because of heat transfer, is estimated as [24]:

$$\dot{E}_{g,air} = \dot{m}_a [(h_{out} - h_{in}) - T_a (s_{out} - s_{in})]_{air}. \quad (11)$$

Exergy loss by the cycle's working fluid ( $\dot{E}_{l,fluid}$ ) during heat transfer process is calculated as [24]:

$$\dot{E}_{g,fluid} = \dot{m}_{4b} [(h_{4b} - h_5) - T_a (s_{4b} - s_5)] - \dot{E}_{g,air}. \quad (12)$$

Temperature  $T_a$  in Eqs. (11) and (12) is in Kelvin.

Finally, the net exergy loss occurring in the Cooler can be obtained by summing exergy gain by cooling air and exergy loss by the working fluid in the Cooler.

$$\dot{E}_{l,Cooler} = \dot{E}_{g,air} + \dot{E}_{l,fluid}. \quad (13)$$

### 6. Assumptions

Following is a list of assumed parameters in this study [24, 26, 27].

1. Energy losses in the pipes are disregarded.
2. Turbine and compressors adiabatic efficiencies are 93 % and 89 % respectively.
3. Heat exchanger effectiveness is 95 % with a minimum pinch point temperature is 5°C for LTR and HTR.
4. A minimum approach of 10°C is used for Cooler.
5. Cycle maximum pressure is 25 MPa.
6. Cycle operates above critical point of the working fluid.

### 7. Model validation

To validate the results produced by the model simulated in Aspen HYSYS, the thermal efficiency of the S-CO<sub>2</sub> RBC is calculated and validated with the published data from Kulhánek and Dostál, Turchi et al. and Padilla et al. [24, 26, 27]. Cycle minimum temperature is considered 32°C to match the condition used in the literature. Fig. 4 represents the plot of thermal efficiencies for turbine inlet temperatures from 350°C to 850°C. It is evident from this plot that the results are in good agreement with the literature, therefore, the same model is used to extend the investigation.

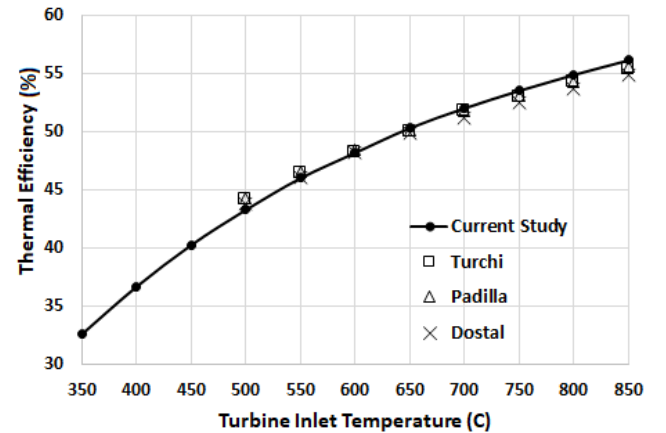


Fig. 4 Validation of results for S-CO<sub>2</sub> RBC with [24, 26, 27]

### 8. Cycle minimum temperature

S-CO<sub>2</sub> RBC is known to achieve maximum efficiency if the conditions at the inlet of compressor C1 are maintained close to its critical point ( $T_{cr} = 31^\circ\text{C}$ ,  $P_{cr} = 7.38$  MPa), which is impossible to attain in the warm or hot regions of the world with significantly higher ambient temperatures. To quantify the drop in the performance of S-CO<sub>2</sub> RBC with increasing minimum temperature, thermal

efficiencies are calculated for a minimum temperature of 40°C and 50°C and plotted in Fig. 5. Thermal efficiency decreases with increasing cycle minimum temperature, as expected. However, the drop in thermal efficiency is large at lower turbine inlet temperatures. For example, in comparison to thermal efficiency with  $T_{\min} = 32^\circ\text{C}$ , data for  $T_{\min} = 40^\circ\text{C}$  show a decrease of nearly 3% and 7.5% in efficiency with  $TIT$  of 850°C and 350°C, respectively. On the other hand, a decline of 6% and 21% is found for  $T_{\min} = 50^\circ\text{C}$  at  $TIT$  of 850°C and 350°C, respectively.

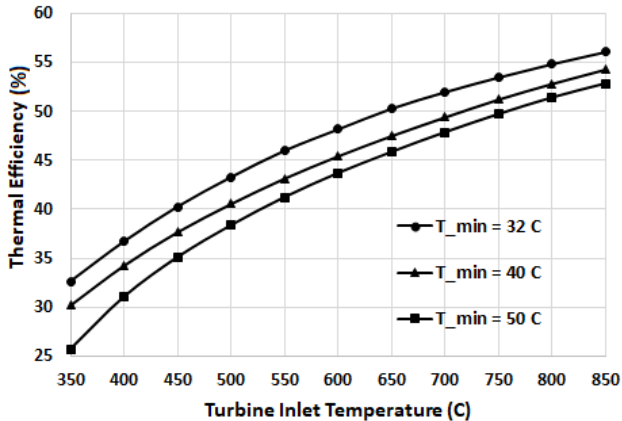


Fig. 5 The effect of cycle minimum temperature on thermal efficiency of S- $\text{CO}_2$  RBC

## 9. Supercritical $\text{CO}_2$ - $\text{C}_7\text{H}_8$ binary mixture RBC

This section discusses the energy and exergy performances of RBC with  $\text{CO}_2$ - $\text{C}_7\text{H}_8$  binary mixture as a working fluid operating above its critical point. The cycle performance is evaluated and compared with the performance of the cycle using pure  $\text{CO}_2$  for the same turbine inlet temperatures and similar ambient conditions. The cycle is investigated with cycle's minimum temperature (at state 5 in Fig. 3) close to 50°C. The underlying idea of using binary

mixture is to raise the critical point of the working fluid to cycle's minimum temperature, therefore, a 96%  $\text{CO}_2$  and 4%  $\text{C}_7\text{H}_8$  composition is selected.

### 9.1. Energy analysis

Energy analyses of supercritical RBC were carried out with  $\text{CO}_2$  and  $\text{CO}_2$ - $\text{C}_7\text{H}_8$  binary mixture at turbine inlet temperatures of 350°C and 400°C. For the comparison purpose, a constant heat of 1MW was supplied to both cycles and keeping the minimum cycle temperature equal to 50°C. Thermal efficiencies and related parameters of the cycles were computed and shown in table 1. It is evident from the data, that the RBC with  $\text{CO}_2$ - $\text{C}_7\text{H}_8$  binary mixture perform much better than RBC with  $\text{CO}_2$  with nearly 11% improvement in thermal efficiency. The net compression work for both cycles is found nearly the same but the turbine output is significantly higher for RBC with  $\text{CO}_2$ - $\text{C}_7\text{H}_8$  binary mixture. It is noteworthy that the net mass flow rate of the working fluid required per megawatt of net power output from the cycle is significantly smaller for RBC operating with  $\text{CO}_2$ - $\text{C}_7\text{H}_8$  binary mixture, which means much smaller turbomachines are needed and ultimately reduced capital cost.

The temperature-entropy diagrams of both cycles with turbine inlet temperature of 400°C are presented in Fig. 6 and Fig. 7. It is observed that the HTR is operating at much higher temperature for the cycle using  $\text{CO}_2$  only. Moreover, the cycle using  $\text{CO}_2$ - $\text{C}_7\text{H}_8$  binary mixture allows uniform and gradual temperature drop in HTR and LTR (refer to temperatures of state points 2, 3 and 4 in Fig. 6 and Fig. 7). Although the equal amount of heat is provided to both cycles (i.e. 1MW), the Heat Source raises the temperature of the working fluid by nearly 120°C for the cycle using  $\text{CO}_2$ - $\text{C}_7\text{H}_8$  binary mixture, on the other hand, a mere 50°C temperature rise occurs in the cycle with 100%  $\text{CO}_2$ . This is because the cycle using pure  $\text{CO}_2$  requires larger mass flowrate than the cycle using  $\text{CO}_2$ - $\text{C}_7\text{H}_8$  binary mixture (refer to Table 1).

Table 1

Energy balance of the RBC operating with pure  $\text{CO}_2$  and  $\text{CO}_2$ - $\text{C}_7\text{H}_8$  binary mixture as a working fluid

$TIT, ^\circ\text{C}$	Heat input, MW	C1 duty, MW	C2 duty, MW	Turbine output, MW	Net Work output, MW	Cooler duty, MW	Net mass flow rate required per MW of Net Work output, kg/sec	Thermal efficiency, %
Working fluid ( $\text{CO}_2$ )								
350	1.00	0.13	0.09	0.48	0.26	0.74	101	25.61
450	1.00	0.15	0.10	0.56	0.31	0.69	58	31.11
Working fluid (96% $\text{CO}_2$ and 4% $\text{C}_7\text{H}_8$ )								
350	1.00	0.12	0.16	0.57	0.29	0.71	22.5	29.29
450	1.00	0.11	0.15	0.60	0.34	0.66	18	33.54

### 9. 2. Exergy analysis

Exergetic performances of the cycles were conducted by calculating the irreversibility losses using model equations from Eq. (3) to Eq. (13). Fig. 8 presents a bar chart showing a component-wise percentage loss in the input exergy due to irreversibilities. In general, for both cycles, net exergy loss occurring in the heat exchangers (Heat Source, Cooler, LTR and HTR) is relatively higher than in the turbomachines (Turbine, Comp C1 and Comp C2). Moreover, the exergy losses occurring in turbomachines by both cycles

are nearly the same, with maximum loss incurs in the Turbine. Exergy loss occurring in the Heat Source is relatively high for the cycle using binary mixture, however, significantly higher exergy loss takes place in HTR for cycle using  $\text{CO}_2$  only. This due to the fact the HTR is operating at higher temperature in the cycle using 100%  $\text{CO}_2$ , moreover, a larger temperature difference exists between its inlets and outlets. Comparing the overall exergetic performance of the two RBC cycles, the cycle using pure  $\text{CO}_2$  as a working fluid shows nearly 5% higher exergy losses than the cycle with  $\text{CO}_2$ - $\text{C}_7\text{H}_8$  binary mixture.

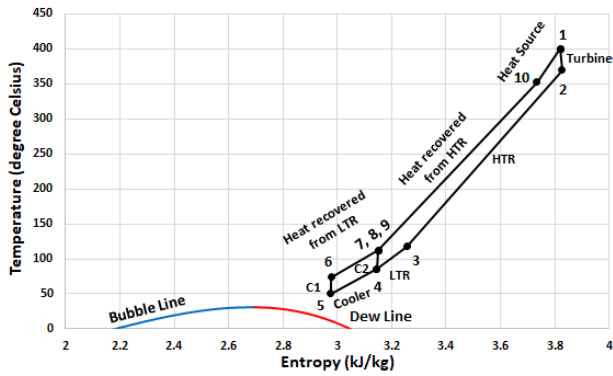


Fig. 6 Temperature-entropy diagram of RBC operating at  $TIT$  of  $400^{\circ}\text{C}$  with 100%  $\text{CO}_2$

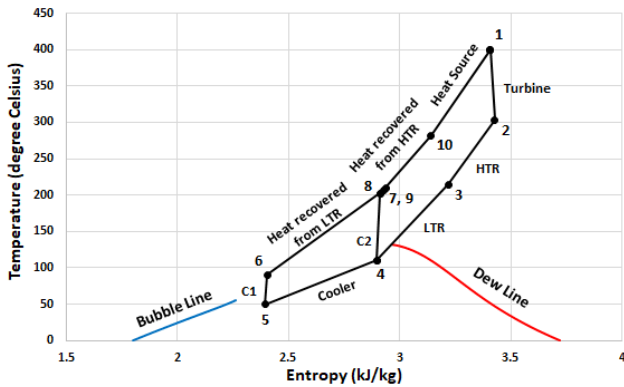


Fig. 7 Temperature-entropy diagram of RBC operating at  $TIT$  of  $400^{\circ}\text{C}$  with 96%  $\text{CO}_2$  and 4%  $\text{C}_7\text{H}_8$

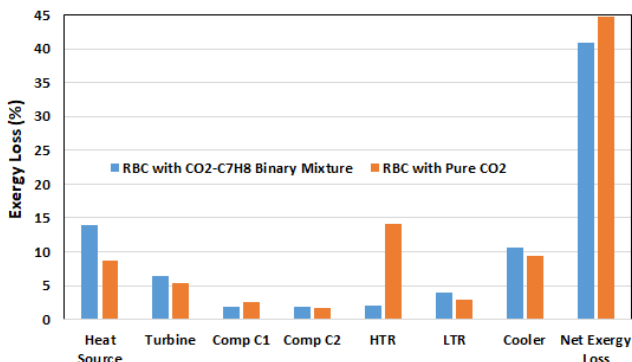


Fig. 8 Component-wise exergy loss in the RBC with pure  $\text{CO}_2$  and  $\text{CO}_2\text{-C}_7\text{H}_8$  binary mixture

## 10. Conclusions

Energy and exergy performances of recompression Brayton cycle was performed. The cycle operated in warm ambient conditions with cycle minimum temperature of about  $50^{\circ}\text{C}$ . 96%  $\text{CO}_2$  and 4% Toluene binary mixture was used as a working fluid for RBC and results were compared with the cycle operating with pure  $\text{CO}_2$ . Key outcomes of the investigation and concluding remarks are as follow:

- RBC with pure  $\text{CO}_2$  offers maximum efficiency if the cycle minimum temperature is maintained close to its critical temperature (i.e.  $31^{\circ}\text{C}$ ).
- Cycle minimum temperature cannot be maintained to  $\text{CO}_2$  critical temperature in warmer regions, and the overall performance of the cycle drops significantly, especially when the source temperatures are low. For example, cycle thermal efficiency decreases by nearly 0.2 points per degree rise in cycle minimum temperature with  $TIT$  of

$850^{\circ}\text{C}$  which rises to 0.32 points when turbine operated at  $350^{\circ}\text{C}$ .

- $\text{CO}_2\text{-C}_7\text{H}_8$  binary mixture provided favourable thermodynamic properties, raising the critical point to desired minimum level. Due to thermodynamic properties of  $\text{C}_7\text{H}_8$ , the cycle maximum temperature was restricted to  $400^{\circ}\text{C}$ .
- When operated RBC with  $\text{CO}_2\text{-C}_7\text{H}_8$  binary mixture, the thermal efficiency improved by nearly 14.5% and 8% with  $TIT$  of  $350^{\circ}\text{C}$  and  $400^{\circ}\text{C}$ , respectively.
- RBC using  $\text{CO}_2\text{-C}_7\text{H}_8$  binary mixture requires much smaller mass flow rate in comparison to RBC using pure  $\text{CO}_2$ .
- Exergy analysis showed that the second law efficiency of the cycle using  $\text{CO}_2\text{-C}_7\text{H}_8$  binary mixture is nearly 60%, whereas, about 55% is found for cycle with pure  $\text{CO}_2$ .

## References

1. Feher, E. G. 1968. The supercritical thermodynamic power cycle, Energy Conversion 8: 85-90. [https://doi.org/10.1016/0013-7480\(68\)90105-8](https://doi.org/10.1016/0013-7480(68)90105-8).
2. Angelino, G. 1968. Carbon dioxide condensation cycles for power production, Journal of Engineering for Power 90: 287-295. <https://doi.org/10.1115/1.3609190>.
3. Dostál, V.; Driscoll, M. J.; Hejzlar, P. 2004. A supercritical carbon dioxide cycle for next generation nuclear reactors, Journal of Engineering for Power, Technical Report MIT-ANP-TR-100: 1-317. <http://hdl.handle.net/1721.1/67671>.
4. Ahn, Y.; Bae, S. J.; Kim, M.; Cho, S. K.; Baik, S.; Lee, J. I.; Cha, J. E. 2015. Review of supercritical  $\text{CO}_2$  power cycle technology and current status of research and development, Nuclear Engineering and Technology 47: 647-661. <https://doi.org/10.1016/j.net.2015.06.009>.
5. Al-Sulaiman, F. A.; Atif, M. 2015. Performance comparison of different supercritical carbon dioxide Brayton cycles integrated with a solar power tower, Energy 82: 61-71. <https://doi.org/10.1016/j.energy.2014.12.070>.
6. Wang, K. A.; He, Y. L.; Zhu, H. H. 2017. Integration between supercritical  $\text{CO}_2$  Brayton cycles and molten salt solar power towers: A review and a comprehensive comparison of different cycle layouts, Applied Energy 195: 819-836. <https://doi.org/10.1016/j.apenergy.2017.03.099>.
7. Lasala, S. A.; Bonalumi, D.; Macchi, E.; Privat, R.; Jaubert, J. N. 2017. The design of  $\text{CO}_2$ -based working fluids for high-temperature heat source power cycles, Energy Procedia 129: 947-954. <https://doi.org/10.1016/j.egypro.2017.09.125>.
8. Manzolini, G.; Binotti, M.; Bonalumi, D.; Invernizzi, C.; Iora P. 2019.  $\text{CO}_2$  mixtures as innovative working fluid in power cycles applied to solar plants. Techno-economic assessment, Solar Energy 181: 530-544. <https://doi.org/10.1016/j.solener.2019.01.015>.
9. Invernizzi, C. M.; van der Stelt, T. 2012. Supercritical and real gas Brayton cycles operating with mixtures of carbon dioxide and hydrocarbons, Proceedings of the Institution of Mechanical Engineers Part A: Journal of Power and Energy 226: 682-693. <https://doi.org/10.1177/0957650912444689>.
10. Invernizzi, C. 2017. Prospects of mixtures as working

- fluids in real-gas Brayton cycles, *Energies* 10: 1-15.  
<https://doi.org/10.3390/en10101649>
11. **Baik, S.; Lee, J. I.** 2018. Preliminary study of supercritical CO<sub>2</sub> mixed with gases for power cycle in warm environments, *Proceedings of the ASME Turbo Expo* 9: GT2018-76386.  
<https://doi.org/10.1115/GT2018-76386>.
  12. **Haroon, M.; Ayub, A.; Sheikh, N. A.; Imran, M.** 2020. Exergetic performance and comparative assessment of bottoming power cycles operating with carbon dioxide-based binary mixture as working fluid, *International Journal of Energy Research* 44: 7957-7973.  
<https://doi.org/10.1002/er.5173>.
  13. **Haroon, M.; Sheikh, N. A.; Ayub, A.; Tariq, R. S.; Baheta, A. T.; Imran, M.** 2020. Exergetic, Economic and Exergo-Environmental Analysis of Bottoming Power Cycles Operating with CO<sub>2</sub>-Based Binary Mixture, *Energies* 13: 1-19.  
<https://doi.org/10.3390/en13195080>.
  14. **Dai, B.; Li, M.; Ma, Y.** 2014. Thermodynamic analysis of carbon dioxide blends with low GWP (global warming potential) working fluids-based transcritical Rankine cycles for low-grade heat energy recovery, *Energy* 64: 942-952.  
<https://doi.org/10.1016/j.energy.2013.11.019>.
  15. **Ng, H. J.; Robinson, D. B.; Ma, Y.** 1978. Equilibrium phase properties of the toluene-carbon dioxide system, *Journal of Chemical and Engineering Data* 23: 325-327.  
<https://doi.org/10.1021/je60079a020>.
  16. **Invernizzi, C. M.; Iora, P.; Manzolini, G.; Lasala, S.** 2017. Thermal stability of n-pentane, cyclo-pentane and toluene as working fluids in organic Rankine engines, *Applied Thermal Engineering* 121: 172-179.  
<https://doi.org/10.1016/j.applthermaleng.2017.04.038>.
  17. **Reaves, J. T.; Griffith, A. T.; Roberts, C. B.** 1998. Critical properties of dilute carbon dioxide + entrainer and ethane + entrainer mixtures, *Journal of Chemical and Engineering Data* 43: 683-686.  
<https://doi.org/10.1021/je9702753>.
  18. **Gao, W.; Yao, M.; Chen, Y.; Li, H.; Zhang, Y.; Zhang, L.** 2019. Performance of s-CO<sub>2</sub> Brayton cycle and organic Rankine cycle (ORC) combined system considering the diurnal distribution of solar radiation, *Journal of Thermal Science* 28: 463-471.  
<https://doi.org/10.1007/s11630-019-1114-8>.
  19. **Maio, D. V. D.; Boccitto, A.; Caruso, G.** 2015. Supercritical carbon dioxide applications for energy conversion systems, *Energy Procedia* 82: 819-824.  
<https://doi.org/10.1016/j.egypro.2015.11.818>.
  20. **Crespi, F.; Gavagnin, G.; Sánchez, D.; Martínez, G. S.** 2017. Supercritical carbon dioxide cycles for power generation: a review, *Applied Energy* 195: 152-183.  
<https://doi.org/10.1016/j.apenergy.2017.02.048>.
  21. **Angelino, G.; Invernizzi, C. M.** 2009. Carbon dioxide power cycles using liquid natural gas as heat sink, *Applied Thermal Engineering* 29: 2935-2941.  
<https://doi.org/10.1016/j.applthermaleng.2009.03.003>.
  22. **Iverson, B. D.; Conboy, T. M.; Pasch, J. J.; Krui-zenga, A. M.** 2013. Supercritical CO<sub>2</sub> Brayton cycles for solar-thermal energy, *Applied Energy* 111: 957-970.  
<https://doi.org/10.1016/j.apenergy.2013.06.020>.
  23. **Siddiqui, M. E.; Almitani, K. H.** 2020. Energy and exergy assessment of s-CO<sub>2</sub> Brayton cycle coupled with a solar tower system, *Processes* 8: 1-23.  
<https://doi.org/10.3390/pr8101264>.
  24. **Padilla, R. V.; Too, Y. C. S.; Benito, R.; Stein, W.** 2015. Exergetic analysis of supercritical CO<sub>2</sub> Brayton cycles integrated with solar central receivers, *Applied Energy* 148: 348-365.  
<https://doi.org/10.1016/j.apenergy.2015.03.090>.
  25. **Besarati, S. M.; Goswami, D. Y.** 2014. Analysis of advanced supercritical carbon dioxide power cycles with a bottoming cycle for concentrating solar power applications, *Journal of Solar Energy Engineering* 136: 1-7.  
<https://doi.org/10.1115/1.4025700>.
  26. **Kulhánek, M.; Dostál, V.** 2011. Thermodynamic analysis and comparison of supercritical carbon dioxide cycles, *Supercritical CO<sub>2</sub> Power Cycle Symposium: Boulder, Colorado, USA*.
  27. **Turchi, C. S.; Ma, Z.; Neises, T. W.; Wanger, M. J.** 2013. Thermodynamic study of advanced supercritical carbon dioxide power cycles for concentrating solar power systems, *Journal of Solar Energy Engineering* 135: 1-7.  
<https://doi.org/10.1115/1.4024030>.

M. E. Siddiqui

#### THERMODYNAMIC PERFORMANCE IMPROVEMENT OF RECOMPRESSION BRAYTON CYCLE UTILIZING CO<sub>2</sub>-C<sub>7</sub>H<sub>8</sub> BINARY MIXTURE

#### S u m m a r y

The article deals with the energy and exergy performance analyses of supercritical carbon dioxide recompression Brayton cycle (S-CO<sub>2</sub> RBC). This cycle is known to offer maximum efficiency when operating near the critical point of CO<sub>2</sub>, which is possible in low ambient temperature environment but not in warm or hot ambient conditions. CO<sub>2</sub>-C<sub>7</sub>H<sub>8</sub> binary mixture is used to improve the thermodynamic performance of the cycle for warmer ambient conditions. The percentage of C<sub>7</sub>H<sub>8</sub> in the mixture is selected according to cycle's minimum temperature, which is assumed 50°C. When using CO<sub>2</sub>-C<sub>7</sub>H<sub>8</sub> binary mixture, the analysis shows that the thermal efficiency of the cycle is improved by nearly 14.5% and 8% for turbine inlet temperatures of 350°C and 400°C, respectively. Moreover, exergetic performance analysis reveals better performance of RBC with CO<sub>2</sub>-C<sub>7</sub>H<sub>8</sub> binary mixture.

**Keywords:** supercritical carbon dioxide, binary mixture, recompression Brayton cycle, energy analysis, exergy analysis, toluene.

Received December 09, 2020

Accepted June 02, 2021

